



Since January 2020 Elsevier has created a COVID-19 resource centre with free information in English and Mandarin on the novel coronavirus COVID-19. The COVID-19 resource centre is hosted on Elsevier Connect, the company's public news and information website.

Elsevier hereby grants permission to make all its COVID-19-related research that is available on the COVID-19 resource centre - including this research content - immediately available in PubMed Central and other publicly funded repositories, such as the WHO COVID database with rights for unrestricted research re-use and analyses in any form or by any means with acknowledgement of the original source. These permissions are granted for free by Elsevier for as long as the COVID-19 resource centre remains active.

A Nonlinear Hysteretic Model for Automated Prediction of Lung Mechanics during Mechanical Ventilation

Cong Zhou^{***}, J. Geoffrey Chase^{**}, Qianhui Sun^{**}, Jennifer Knopp^{**}

^{*}School of Civil Aviation, Northwestern Polytechnical University, China (e-mail: cong.zhou@nwpu.edu.cn)

^{**}Department of Mechanical Engineering; Dept of Mechanical Eng, Centre for Bio-Engineering, University of Canterbury Christchurch, New Zealand, (e-mail: geoff.chase@canterbury.ac.nz; qianhui.sun@pg.canterbury.ac.nz; jennifer.knopp@canterbury.ac.nz)

Abstract: Mechanical ventilation (MV) is core intensive care unit (ICU) therapy during the Covid-19 pandemic. Optimising MV care to a specific patient with respiratory failure is difficult due to inter- and intra- patient variability in lung mechanics and condition. The ability to accurately predict patient-specific lung response to a change in MV settings would enable semi-automated care and significantly improve the efficiency of MV monitoring and care. It has particular emphasis when considering MV care required to treat Covid-19 patients, who require longer MV care, where patient-specific care can reduce the time on MV required.

This study develops a nonlinear smooth hysteresis loop model (HLM) able to capture the essential lung dynamics in a patient-specific fashion from measured ventilator data, particularly for changes of compliance and inflection points of the pressure-volume loop. The automated (no human input) hysteresis loop analysis (HLA) method is applied to identify HLM model parameters, enabling automated digital cloning to create a virtual patient model to accurately predict lung response at a specified positive end expiratory pressure (PEEP) level, as well as in response to the changes of PEEP. The performance of this automated digital cloning approach is assessed using clinical data from 4 patients and 8 recruitment maneuver (RM) arms.

Validation results show the HLM-based hysteresis loops identified using HLA match clinical pressure-volume loops very well with root-mean-square (RMS) errors less than 2% for all 8 data sets over 4 patients, validating the accuracy of the developed HLM in capturing the essential lung physiology and respiratory behaviours at different patient conditions. More importantly, the patient-specific digital clones at lower PEEP levels accurately predict lung response at higher PEEP levels with predicted peak inspiratory pressure (PIP) errors less than 2% in average. In addition, the resulted additional lung volume V_{frc} obtained with PEEP changes are predicted with average absolute difference of 0.025L. The overall results validate the versatility and potential of the developed HLM for delineating changes of nonlinear lung dynamics, and its capability to create a predictive virtual patient with use of HLA for future treatment personalization and optimisation in MV therapy.

Copyright © 2020 The Authors. This is an open access article under the CC BY-NC-ND license (<http://creativecommons.org/licenses/by-nc-nd/4.0>)

Keywords: Nonlinear Modelling; Hysteresis Model; Hysteresis loop analysis; Virtual Patient; Mechanical Ventilation; Lung mechanics.

1. INTRODUCTION

Mechanical ventilation (MV) is core therapy for patient suffering respiratory failure and acute respiratory distress syndrome (ARDS) in intensive care unit (ICU), currently one of the major way to support lives of Covid-19 patients (Mahase, 2020). However, MV is invasive and may cause a further lung injury and higher mortality if MV settings are poorly suited to the patients (Major et al., 2018). Accurate prediction of patient-specific lung response to the changes of MV settings, such as peak positive end expiratory pressure (PEEP) would enable a more confident and efficient MV design, minimizing the risk of barotrauma and volutrauma (Langdon et al., 2017). In addition, an optimised MV care would also reduce the treatment time of patient on a ventilator, which is critical for improving the capacity of health systems to provide adequate MV during the Covid-19 pandemic.

Current studies of basis functions have shown good modelling and predicting outcome of lung mechanics and airway pressure based on a single compartment linear lung model (Langdon et al., 2017, Morton et al., 2018, Morton et al., 2019). These methods are built on the assumptions of data mode, changes of specific elastance and resistance shapes, lacking of ability to fully represent the lung mechanics, such as the additional lung volume or dynamic functional residual capacity (V_{frc}).

Hence, this work focuses on the development of a nonlinear hysteresis loop model (HLM) from the perspective of mechanical-physiological relevance for the dynamic respiratory system. The new HLM is able to capture the essential lung mechanics for creating a patient-specific virtual patient in an automated fashion. Identification and prediction methods are also developed with clinical measurements at a low PEEP level. The performance of the proposed model and methods for predicting lung dynamics at higher PEEP levels

are investigated. In addition, the additional lung volume during the change of PEEP is also predicted using the created virtual patient model.

2. METHOD

2.1 Hysteresis Loop Model for Lung Respiratory

The key features for lung respiratory dynamics include the recruitment of alveoli and alveolar distension in inspiratory, as well as the recoil of lung elastance in expiratory. The identifiable HLM is thus proposed with a linear spring, K_e , to represent the lung tissue elastance, and two nonlinear hysteretic spring, K_{h1} and K_{h2} , for alveolar expanding elastance during inspiration and expiration, respectively. To account for the end-inspiratory plateau pressure, a nonlinear element controlled by energy absorption is also added to the inspiration hysteretic spring. Thus, the dynamic equation of motion for the proposed model is defined:

$$\ddot{V} + R\dot{V} + K_e V + K_{h1} V_{h1} + K_{h2} V_{h2} = f_V(t) + PEEP \quad (1)$$

where V is the volume of air delivered to lungs, V_{h1} and V_{h2} are hysteretic volume response during inspiration and expiration, respectively. R is the airway resistance, PEEP is the positive end-expiratory pressure, and $f_V(t)$ is the steady-state input force. The nonlinear stiffness, $K(t)$, for a breath can thus be defined in a differential form (Zhou and Chase, 2020):

$$K(t) = \frac{df_r}{dV} = K_e + K_{h1} \frac{\dot{V}_{h1}}{\dot{V}} + K_{h2} \frac{\dot{V}_{h2}}{\dot{V}} \quad (2)$$

Thus, the change of nonlinear stiffness is determined by the two hysteretic springs $K_{h1} \frac{\dot{V}_{h1}}{\dot{V}}$ and $K_{h2} \frac{\dot{V}_{h2}}{\dot{V}}$. Particularly, the inspiratory hysteretic spring is defined:

$$\frac{\dot{V}_{h1}}{\dot{V}} = f_{sign}^+ \left(1 - \left(\frac{V_{h1}}{V_{m1}} \right)^2 - \delta \left(\frac{E_{h1}}{E_{m1}} \right)^q \right) + K_c f_{sign}^- \quad (3)$$

where V_{m1} is the lower deflection point, δ controls the end-inspiratory stiffness for plateau pressure, E_{h1} is the dissipated energy due to inspiratory hysteresis, q controls the smoothness of plateau stiffness and E_{m1} is the maximum energy without inspiratory pause at the peak alveolar pressure. K_c controls stiffness changes from inspiration to expiration with defined signum functions f_{sign}^+ and f_{sign}^- :

$$f_{sign}^+ = 0.5 * \left(1 + \text{sign}(V_{h1}\dot{V}) \right) \quad (4)$$

$$f_{sign}^- = 0.5 * \left(1 - \text{sign}(V_{h1}\dot{V}) \right) \quad (5)$$

The expiratory hysteretic spring is defined with a similar curve shape to inspiration for alveolar derecruitment:

$$\frac{\dot{V}_{h2}}{\dot{V}} = f_{sign}^- \left(1 - \left(\frac{V_{h2}}{V_{m2}} \right)^2 \right) \quad (6)$$

where V_{m2} is the upper deflection point. Therefore, ten (10) parameters, including K_e , K_{h1} , K_{h2} , R , V_{m1} , V_{m2} , E_{m1} , K_c , q and δ are defined to model the lung hysteresis mechanics using the proposed HLM.

2.2 Identification

The goal of section 2.2 is to create a virtual patient at a low PEEP level based on the identification of the proposed HLM

with the ability to predict patient lung dynamics at higher PEEP levels. The identification process can be implemented in an automated fashion without requiring human input, including:

- HLA identification of K_e , K_{h1} , K_{h2} , V_{m1} , V_{m2} and K_c ;
- Calculation of R and f_V ;
- Forward simulation to identify E_{m1} and q .

In particular, HLA is an automated algorithm of identifying the change of slopes and breakpoints for a hysteresis loop (Zhou et al., 2015, Zhou et al., 2017a, Zhou et al., 2017b). The measured PV loop is divided into an inspiratory and expiratory half cycles using the turning point T_{max} at the maximum volume point, shown in Fig 1. The inspiration half cycle is then approximated using two segments with identified stiffness k_1 , k_2 and the breakpoint V_{m1} for inspiration. Similarly, the expiration half cycle is segmented with stiffness k_3 , k_4 and the breakpoint V_{m2} in HLA.

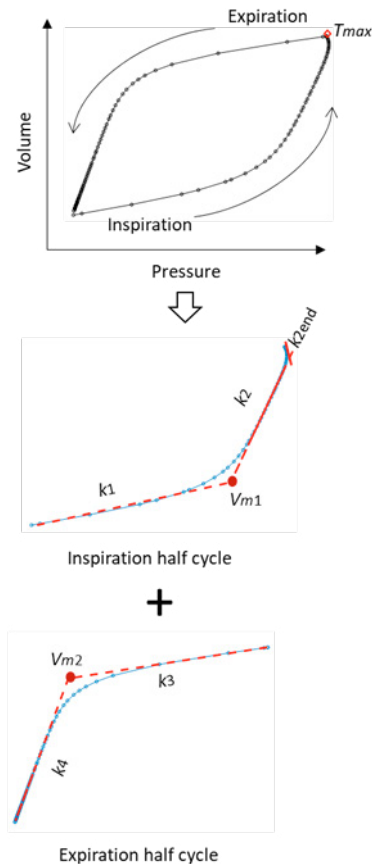


Fig. 1. HLA identification of PV loop

The identified stiffnesses in HLA can thus be used to calculate the model parameters K_e , K_{h1} , K_{h2} and K_c :

$$K_e = k_2 \quad (7)$$

$$K_{h1} = k_1 - k_2 \quad (8)$$

$$K_{h2} = k_3 - k_4 \quad (9)$$

$$K_c = \frac{k_4 - k_2}{k_1 - k_2} \quad (10)$$

The end-inspiratory parameter δ can also be calculated:

$$\delta = \frac{k_4 - k_{2end}}{k_1 - k_2} \quad (11)$$

where k_{2end} is the end-inspiratory stiffness identified in HLA shown in Fig 1.

A steady-state harmonic input force is assumed as the input force, defined:

$$f_V(t) = (k_1 + k_3)\xi(V_{max} - V_{min})\sin\left(\sqrt{\frac{k_1+k_3}{2}} * t + \frac{\pi}{2}\right) \quad (12)$$

where V_{max} and V_{min} are the maximum and minimum volume in the PV loop, respectively. ξ is the damping ratio. The resistance parameter R can then be calculated:

$$R = 2\xi\sqrt{\frac{k_1+k_3}{2}} \quad (13)$$

Finally, both the maximum energy parameter E_{m1} without considering plateau pressure and the smoothness parameter q can be obtained using forward simulation with the identified V_{m1} , K_e , K_{h1} and K_{h2} for inspiratory half cycle.

2.3 Prediction

In the identified HLM, the parameters K_{h1} , K_{h2} , R , V_{m2} , E_{m1} , K_c , q and δ are fixed as constants, while the lung tissue elastance K_e is updated as PEEP changes. Particularly, a pair of linear and parabolic shaped basis functions (Morton et al., 2018, Morton et al., 2019) are defined to the “post-yielding” ratio α representing the change of stiffness from alveolar recruitment to distention in the HLM:

$$\alpha = \frac{K_e}{k_1} = E_1 * PEEP + E_2 * \left(2 - \frac{130}{k_1} - \frac{PEEP}{k_1}\right)^2 \quad (14)$$

where E_1 is the coefficient for distention basis function and E_2 is the coefficient for recruitment basis function. To calculate E_1 and E_2 in Equation (14), the identified K_{e1} and k_1 at the first low PEEP level, PEEP1, can provide

$$\frac{K_{e1}}{k_1} = E_1 * PEEP1 + E_2 * \left(2 - \frac{130}{k_1} - \frac{PEEP1}{k_1}\right)^2 \quad (15)$$

In addition, the maximum value for “post-yielding” ratio α is equal to 1 at the upper limit volume, yielding:

$$1 = E_1 * k_1 \left(2 - \frac{130}{k_1}\right) \quad (16)$$

Combining Equations (15) and (16) to solve:

$$E_1 = \frac{1}{k_1 \left(2 - \frac{130}{k_1}\right)} \quad (17)$$

$$E_2 = \frac{\frac{K_{e1}}{k_1} - E_1 * PEEP1}{\left(2 - \frac{130}{k_1} - \frac{PEEP1}{k_1}\right)^2} \quad (18)$$

In addition, the prediction of V_{m1} can also be determined based on changes of the transition radius from alveolar recruitment to distention.

3. CLINICAL DATA

Clinical data of 4 patients and 8 staircase recruitment maneuver (RM) from the pilot CURE trial conducted at Christchurch Hospital ICU in 2016 are used to validate the modelling accuracy of the developed HLM, as well as the ability of the created virtual patient to predict lung response forward as PEEP changes (Davidson et al., 2014). The New

Zealand Southern Regional Ethics Committee granted ethics approval for this pilot trial. Pressure and flow data were recorded at a sampling rate of 50Hz from a Puritan Bennett 840 ventilator (Covidien Boulder, CO, USA). Patient demographics are presented in Table 1.

Table 1. Patient demographics.

| Patient | Sex | Age | Length of MV | Clinical Diagnostic |
|---------|--------|-----|--------------|-------------------------|
| 1 | Male | 33 | 23 days | Peritonitis |
| 2 | Male | 77 | 24 days | Legionella Pneumonia |
| 3 | Male | 61 | 23 days | Staphylococcus Aureus |
| 4 | Female | 73 | 2 days | Streptococcus Pneumonia |

Each patient was ventilated with two pairs of RM, and each pair of RM includes a staircase increase in PEEP changes followed by a staircase decrease changes of PEEP. The method validation focuses on the two increasing staircase (Arm1 and Arm3) of RM for each patient, thus giving 8 data sets. Table 2 shows the details of PEEP changes for each data set of the 4 patient. Note the set value for PEEP in ventilator are not necessary matched by the real PEEP level performed in patient response. The median values across all breaths samples for each PEEP level are given in Table 2.

Table 2. PEEP changes over increasing staircase of RM.

| Patient | Data Set | PEEP | | | | |
|---------|----------|------|------|------|------|------|
| | | 1 | 2 | 3 | 4 | 5 |
| 1 | Arm1 | 11.2 | 15.5 | 19.5 | 23.5 | 27.5 |
| | Arm3 | 11.7 | 15.4 | 20.1 | 23.7 | 27.6 |
| 2 | Arm1 | 16.8 | 20.3 | 24.8 | 27.4 | 30 |
| | Arm3 | 13.3 | 16.4 | 20.6 | 24.6 | 27.8 |
| 3 | Arm1 | 12.9 | 16.9 | 20.6 | 24.1 | 27 |
| | Arm3 | 12.9 | 16.9 | 21 | 25 | 27 |
| 4 | Arm1 | 16.9 | 20.9 | 24.9 | 28.9 | 30.8 |
| | Arm3 | 12.9 | 17 | 20.9 | 25 | 29 |

4. RESULTS

4.1 Identification and Model Fitting

HLA algorithm is applied to the constructed PV loop to identify the values of k_1 , k_2 , k_3 , k_4 , V_{m1} and V_{m2} . Fig. 2 shows an example of HLA identification at PEEP1 for Patient 1, Arm 1. It can be seen that the divided linear segments fit the measured PV loop very well, with structural changes or breakpoints also well identified for each half cycle. Model parameters K_e , K_{h1} , K_{h2} , R , V_{m1} , V_{m2} , E_{m1} , K_c , q and δ for HLM can then be calculated and identified based on HLA results.

With the identified model parameters, the hysteresis PV loop can be simulated and compared to the clinical hysteresis measured at PEEP1 to validate the identification accuracy and HLM performance for representing the real nonlinear lung

hysteresis dynamics. Fig. 3 compares the HLM modelling response to the clinical response for Patient 1, Arm1, showing a very good match to the clinical data with very low PIP error of 0.4% and RMS error of 1.2%.

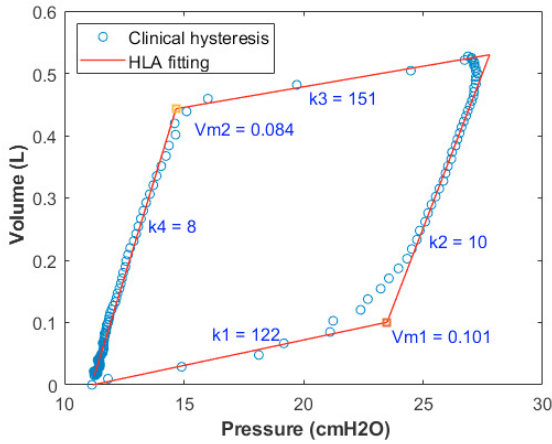


Fig. 2. HLA identification at PEEP1 for Patient 1, Arm1.

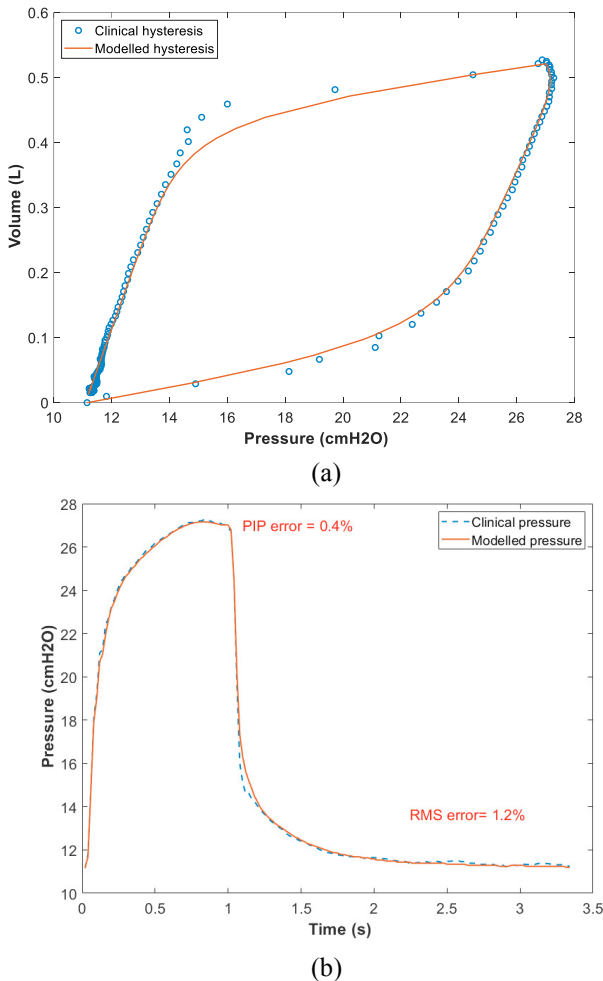


Fig. 3. Compare clinical and modelled response at PEEP1 for Patient 1, Arm1, with (a) hysteresis PV loop and (b) pressure.

The PIP errors and RMS errors for all 8 data sets are listed in Table 3, showing all absolute PIP error are less than 1.4% and RMS errors less than 1.7%, all of which validate the accuracy

of the identification and modelling accuracy. The overall results validates the accuracy of identification and HLM modelling for capturing the essential lung physiology and respiratory behaviours at different patient conditions.

Table 3. Absolute PIP and RMS errors for all patients and sets.

| Patient | Set | PIP error | RMS error |
|---------|------|-----------|-----------|
| 1 | Arm1 | -0.4% | 1.2% |
| | Arm3 | -0.2% | 1.7% |
| 2 | Arm1 | -0.8% | 1.1% |
| | Arm3 | -1.4% | 1.3% |
| 3 | Arm1 | 0.1% | 1.5% |
| | Arm3 | -0.4% | 1.5% |
| 4 | Arm1 | 1.1% | 1.5% |
| | Arm3 | -0.3% | 1.7% |

4.2 Prediction

The identified HLM at PEEP1 is combined with the prediction functions to predict the higher PEEP levels (PEEP2-5). More specifically, this virtual patient model created at PEEP1 provides not only one PEEP step higher (PEEP2) response prediction but also two (PEEP3), three (PEEP4) and four (PEEP5) steps ahead response with only using PEEP1 measurements.

Fig. 4 shows a prediction example for comparing the predicted hysteresis to the clinical measurements at PEEP2-5 for Patient1, Arm1. The predicted PIP errors for all 8 data sets of the 4 patients are listed in Table 4. It shows 57 out of 64 error values are less than 3%. The maximum absolute PIP error is 5.3% from Patient 2 who shows a negative compliance at PEEP1 and PEEP2 while volume is increasing known as spontaneously breathing (SB) (Damanhuri et al., 2016). This SB results in a relatively larger error in predicting accurate values of elastance and response.

However, the accuracies for Patient 2 at the highest PEEP (PEEP5) are very good, while the errors for other 3 patients are also very low with the maximum errors of 2.9% for PIP. These results show the unique capability of the created virtual patient for predicting both small and very large PEEP intervals using only one PEEP measurement.

Table 4. Predicted PIP errors at PEEP2-5 for all patients and data sets.

| Patient | Data Set | PEEP | | | |
|---------|----------|-------|-------|-------|-------|
| | | 2 | 3 | 4 | 5 |
| 1 | Arm1 | 2.9% | 3.1% | 1.2% | -1.5% |
| | Arm3 | -1.1% | 3.6% | 3.9% | 1.3% |
| 2 | Arm1 | -5.3% | 1.9% | 0.2% | -1.6% |
| | Arm3 | -4.4% | 2.4% | 5.1% | 2.2% |
| 3 | Arm1 | 0.4% | -0.3% | -0.5% | 2.9% |
| | Arm3 | 2.3% | 0.7% | 0.9% | 0.3% |
| 4 | Arm1 | 1.0% | 0.9% | 2.7% | 2.6% |
| | Arm3 | -0.1% | 0.6% | 1.9% | 1.6% |

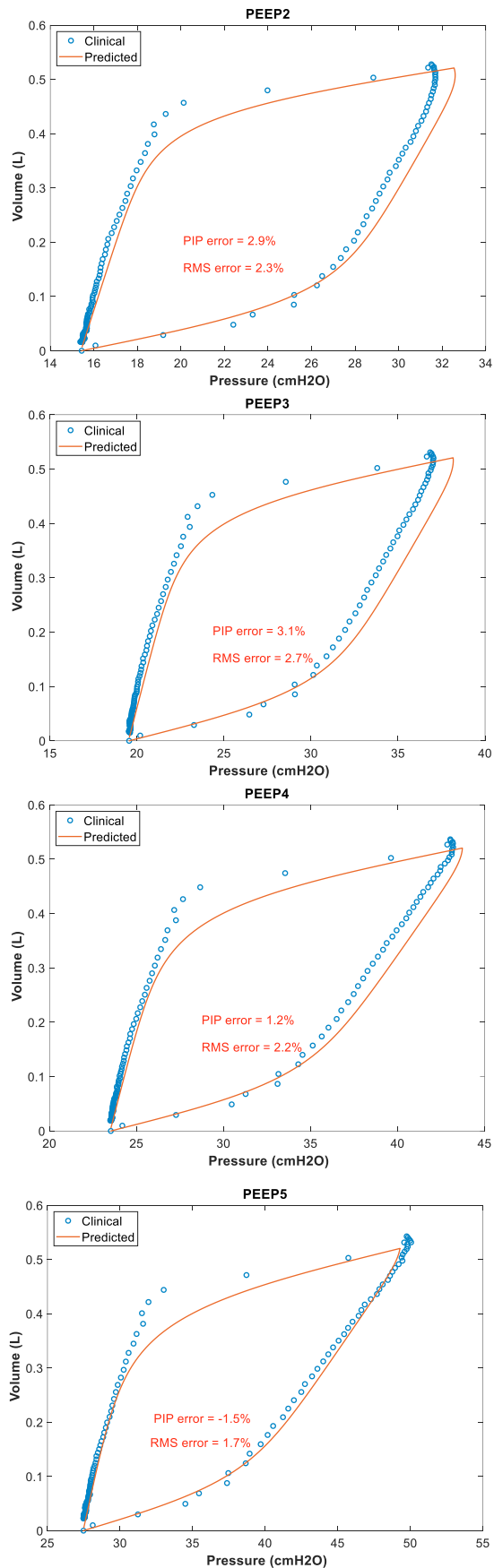


Fig. 4. Response prediction to PEEP2-5 for Patient 1, Arm1.

Finally, the change of V_{frc} due to change of PEEP can be readily simulated using the predictive virtual patient. The predicted absolute V_{frc} errors for all data sets are listed in Table 5. The maximum errors is 0.096L again from Patient 2 as should be expected due to the maximum PIP errors. However, 20 out of 32 predicted errors are less than 0.025L, which is 5% of a normal ventilated tidal volume (0.5L) (Salzer, 2007), and 30 out of 32 are less than 0.05L.

Table 5. Predicted V_{frc} (L) for all patients and data sets.

| Patient | Set | PEEP | | | |
|---------|------|-------|-------|-------|-------|
| | | 2 | 3 | 4 | 5 |
| 1 | Arm1 | 0.006 | 0.015 | 0.028 | 0.026 |
| | Arm3 | 0.007 | 0.023 | 0.012 | 0.022 |
| 2 | Arm1 | 0.018 | 0.017 | 0.004 | 0.046 |
| | Arm3 | 0.061 | 0.096 | 0.044 | 0.033 |
| 3 | Arm1 | 0.031 | 0.007 | 0.020 | 0.012 |
| | Arm3 | 0.046 | 0.044 | 0.045 | 0.021 |
| 4 | Arm1 | 0.017 | 0.016 | 0.014 | 0.017 |
| | Arm3 | 0.032 | 0.005 | 0.009 | 0.004 |

5. CONCLUSIONS

This work proposes an automated modelling approach based on a new developed HLM to predict the change of lung response to the change PEEP levels in a patient-specific fashion. Identification and modelling results at the low PEEP level show a very good match of the clinical and simulation hysteresis, which thus validates the identification accuracy and model efficiency. More importantly, the created virtual patient model with the proposed prediction functions is able to provide a very accurate prediction of both pressure and V_{frc} at higher PEEP levels for the 4 patients. The developed algorithm requires no human-intervention, eliminating the potential subjective uncertainty due to the variations of clinician skills.

REFERENCES

Damanhuri, N. S., Chiew, Y. S., Othman, N. A., Docherty, P. D., Pretty, C. G., Shaw, G. M., Desai, T. & Chase, J. G. (2016). Assessing respiratory mechanics using pressure reconstruction method in mechanically ventilated spontaneous breathing patient. *Computer methods and programs in biomedicine*, 130, 175-185.

Davidson, S. M., Redmond, D. P., Laing, H., White, R., Radzi, F., Chiew, Y. S., Poole, S. F., Damanhuri, N. S., Desai, T. & Shaw, G. M. (2014). Clinical Utilisation of Respiratory Elastance (CURE): Pilot trials for the optimisation of mechanical ventilation settings for the critically ill. *IFAC Proceedings Volumes*, 47, 8403-8408.

Langdon, R., Docherty, P. D., Chiew, Y. S. & Chase, J. G. (2017). Extrapolation of a non-linear autoregressive model of pulmonary mechanics. *Mathematical biosciences*, 284, 32-39.

- Mahase, E. 2020. Covid-19: most patients require mechanical ventilation in first 24 hours of critical care. British Medical Journal Publishing Group.
- Major, V. J., Chiew, Y. S., Shaw, G. M. & Chase, J. G. (2018). Biomedical engineer's guide to the clinical aspects of intensive care mechanical ventilation. *Biomedical engineering online*, 17, 169.
- Morton, S. E., Dickson, J., Chase, J. G., Docherty, P., Desai, T., Howe, S. L., Shaw, G. M. & Tawhai, M. (2018). A virtual patient model for mechanical ventilation. *Computer Methods and Programs in Biomedicine*, 165, 77-87.
- Morton, S. E., Knopp, J. L., Chase, J. G., Möller, K., Docherty, P., Shaw, G. M. & Tawhai, M. (2019). Predictive virtual patient modelling of mechanical ventilation: impact of recruitment function. *Annals of biomedical engineering*, 47, 1626-1641.
- Salyer, S. W. (2007). *Essential emergency medicine: for the healthcare practitioner*, Elsevier Health Sciences.
- Zhou, C., Chase, J. G., Rodgers, G. W., Tomlinson, H. & Xu, C. (2015). Physical Parameter Identification of Structural Systems with Hysteretic Pinching. *Computer-Aided Civil and Infrastructure Engineering*, 30, 247-262.
- Zhou, C., Chase, J. G., Rodgers, G. W. & Iihoshi, C. (2017a). Damage assessment by stiffness identification for a full-scale three-story steel moment resisting frame building subjected to a sequence of earthquake excitations. *Bulletin of Earthquake Engineering*, 15, 5393-5412.
- Zhou, C., Chase, J. G., Rodgers, G. W. & Xu, C. (2017b). Comparing model-based adaptive LMS filters and a model-free hysteresis loop analysis method for structural health monitoring. *Mechanical System and Signal Processing*, 84, 384-398.
- Zhou, C. & Chase, J. G. (2020). A new pinched nonlinear hysteretic structural model for automated creation of digital clones in structural health monitoring. *Structural Health Monitoring*, 1475921720920641.